The Journal of Physical Chemistry A

 VOLUME 102, NUMBER 7, FEBRUARY 12, 1998

ARTICLES

Molecular Dynamics Simulation of $Li^+BF_4^-$ in Ethylene Carbonate, Propylene Carbonate, and Dimethyl Carbonate Solvents

Jean-Christophe Soetens,† Claude Millot,* and Bernard Maigret

Laboratoire de Chimie Théorique, URA CNRS no. 510, Boulevard des Aiguillettes, BP 239, 54506 Vandoeuvre lès Nancy Cedex, France

Received: July 28, 1997; In Final Form: November 24, 1997

Molecular dynamics simulations of $Li^+BF_4^-$ in liquid ethylene carbonate, propylene carbonate, and dimethyl carbonate at low concentration are reported. Structural, thermodynamical, and dynamical properties have been obtained at 323 and 348 K in ethylene carbonate, 298 and 323 K in propylene carbonate, and 298 K in dimethyl carbonate. The diffusion coefficient of the lithium cation is found to be very similar in the three solvents ($(0.3-0.6) \times 10^{-9}$ m^2 s^{-1} in this temperature range). This behavior is linked to the structure of the first solvation shell, which contains four strongly bound solvent molecules in a tetrahedral arrangement in all three cases. No exchange of solvent molecules between the first and the second solvation shells of the lithium ion have been observed during the 100-ps simulations. In the three carbonates, the fluoroborate ion is bound to 19 or 20 solvent molecules in the first solvation shell, the coordination shell being much less structured than in the case of the lithium ion, and the diffusion coefficient exhibits a more significant solvent and temperature dependence.

I. Introduction

Solutions of lithium salts in liquid propylene carbonate (PC), ethylene carbonate (EC), and dimethyl carbonate (DMC) or their mixtures have considerable industrial interest due to their use as electrolytes in rechargeable lithium batteries.[1] Such solvents and their mixtures have proved to be among the most efficient in terms of battery cyclability,[2] and the analysis of the electrolyte physical properties is a necessary step in the understanding of the differences between the electrolytes.

Molecular dynamics simulations are often used to characterize the behavior of electrolyte solutions. Many works concern aqueous solutions[3−7] or aqueous solutions near an electrode.[8] In rechargeable lithium batteries, either liquid or polymer electrolytes are used industrially. In this field, molecular dynamics simulations have so far concerned polymer electrolytes such as poly(ethylene oxide)-like systems.[9−13]

In this work, we focus our attention on the structural and dynamical properties of dilute solutions of lithium fluoroborate ($LiBF_4$) in liquid EC, PC, and DMC. For that purpose we have undertaken molecular dynamics (MD) simulations of one $Li^+-BF_4^-$ ion pair in liquid EC, PC, and DMC at different temperatures. The details of the simulations are given in section II. In section III, we present and discuss our results concerning the structure of the first solvation shell around the ions, the solvation energies, and the ionic diffusion.

II. Simulation Details

Intermolecular interactions are described by atom−atom Lennard-Jones 12−6 (LJ) and Coulomb interactions. The optimized parameters for liquid-phase simulation (OPLS) LJ

* Corresponding author.
† Present address: Laboratoire de Physico-Chimie Moléculaire (LPCM), Université de Bordeaux I, 351 Cours de la Libération, 33405 Talence Cedex, France.

S1089-5639(97)02457-2 CCC: $15.00
Published on Web 01/27/1998

TABLE 1: van der Waals Parameters and Partial Charges Used in the Intermolecular Potentials for Ethylene Carbonate (EC), Propylene Carbonate (PC), and Dimethyl Carbonate (DMC). The Labels of Atoms Are Defined in Figure 1

molecule	atom	σ/Å	ϵ/(kcal mol^{-1})	q/e
EC	O_1	2.96	0.210	−0.6452
	C_1	3.75	0.105	1.0996
	O_{2-3}	3.00	0.170	−0.4684
	C_{2-3}	3.50	0.066	0.0330
	H_{1-4}	2.50	0.030	0.1041
PC	O_1	2.96	0.210	−0.6378
	C_1	3.75	0.105	1.0489
	O_2	3.00	0.170	−0.4509
	O_3	3.00	0.170	−0.4120
	C_2	3.50	0.066	−0.0040
	C_3	3.50	0.066	0.0832
	C_4	3.50	0.066	−0.3264
	H_{1-6}	2.50	0.030	0.1165
DMC	O_1	2.96	0.210	−0.6774
	C_1	3.75	0.105	1.0864
	O_{2-3}	3.00	0.170	−0.4478
	C_{2-3}	3.50	0.066	−0.1561
	H_{1-6}	2.50	0.030	0.1331
Li^+		1.46	0.191	1.0000
BF_4^-	B	0.00	0.000	0.9756
	F	3.00	0.068	−0.4939

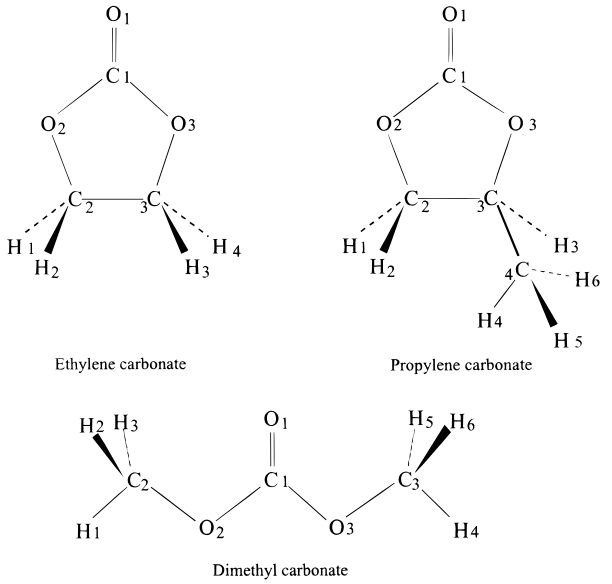

Figure 1. Structure and definition of the atomic labels for the ethylene carbonate (EC), propylene carbonate (PC), and dimethylcarbomate (DMC) molecules.

parameters of Carlson et al.[14] are used (with geometric average combination rules). The electrostatic interactions are modeled using partial atomic charges. For the carbonate molecules and the BF_4^- ion, the charges are fitted to reproduce the electrostatic potential around the molecule obtained from ab initio calculation using the Hartree−Fock 6-31G** wave functions by means of the program GRID.[15] LJ parameters for lithium and fluorine atoms are fitted to reproduce Hartree−Fock 6-31G** ab initio calculations on $Li(EC)_{n=1,2}^+$ and $BF_4(EC)_1^-$ clusters. The list of parameters is given in Table 1, and the molecules involved are sketched in Figure 1. Molecular flexibility is taken into account through the inclusion of an intramolecular force field. A previous study has shown that among the Amber,[16] CVFF,[17] and CFF91[18,19] force fields, CFF91 is the only one leading to acceptable agreement with the minimum energy structures of EC, PC, and DMC as well as their barriers to conformational inversion.[20] Consequently, the CFF91 forcefield is used to describe the intramolecular interactions of the three carbonate molecules. For PC, we consider a racemic mixture of enantiomers. The tetrahedral BF_4^- ion is treated as rigid

TABLE 2: Results of Molecular Dynamics Simulations of Dilute Solutions of One $Li^+BF_4^-$ Ion Pair in Three Liquid Carbonate Solvents (214 Molecules)[a]

	EC 323 K	EC 348 K	PC 298 K	PC 323 K	DMC 298 K
box edge/Å	28.90	29.11	31.29	31.53	31.14
equilibration/ps	125	10	60	25	40
sampling/ps	100	100	100	100	70
T/K	322.7	347.8	297.5	322.6	297.9
pressure/10^5 Pa	1727	1271	612	427	72
energies/kJ mol^{-1}					
solution					
U_{tot}	−16205	−15813	−16100	−15387	−11713
Li^+−solvent					
U_{pot}	−1012.3	−997.1	−990.0	−995.5	−948.0
U_{el}	−1052.7	−1035.9	−1029.9	−1030.9	−993.2
U_{rep}	76.0	74.0	75.3	69.8	81.5
U_{dis}	−35.6	−35.1	−35.4	−34.4	−36.7
BF_4^-−solvent					
U_{pot}	−468.8	−466.5	−459.1	−454.7	−416.7
U_{el}	−452.9	−452.0	−445.1	−438.5	−401.9
U_{rep}	52.6	51.5	48.4	44.5	38.5
U_{dis}	−68.5	−66.0	−62.4	−60.6	−58.3
diffusion coefficient/					
10^{-9} m^2 s^{-1}					
Li^+ (VAC)	0.37	0.46	0.42	0.58	0.44
Li^+ (MSD)	0.47	0.40	0.40	0.51	0.51
BF_4^- (VAC)	0.43	0.95	0.24	0.78	1.42
BF_4^- (MSD)	0.60	1.00	0.34	1.08	1.60

[a] T is the average temperature. U_{tot} is the average total potential energy of the solution, U_{pot}, U_{el}, U_{rep}, and U_{dis} are potential energy and electrostatic, repulsion, and dispersion components of the potential energy of the ions in the solutions. Pressure and total potential energy U_{tot} include the usual corrections due to the truncation of Lennard-Jones interactions at half the box edge. Self-diffusion coefficients are obtained from the velocity autocorrelation function (VAC) and mean square displacement (MSD).

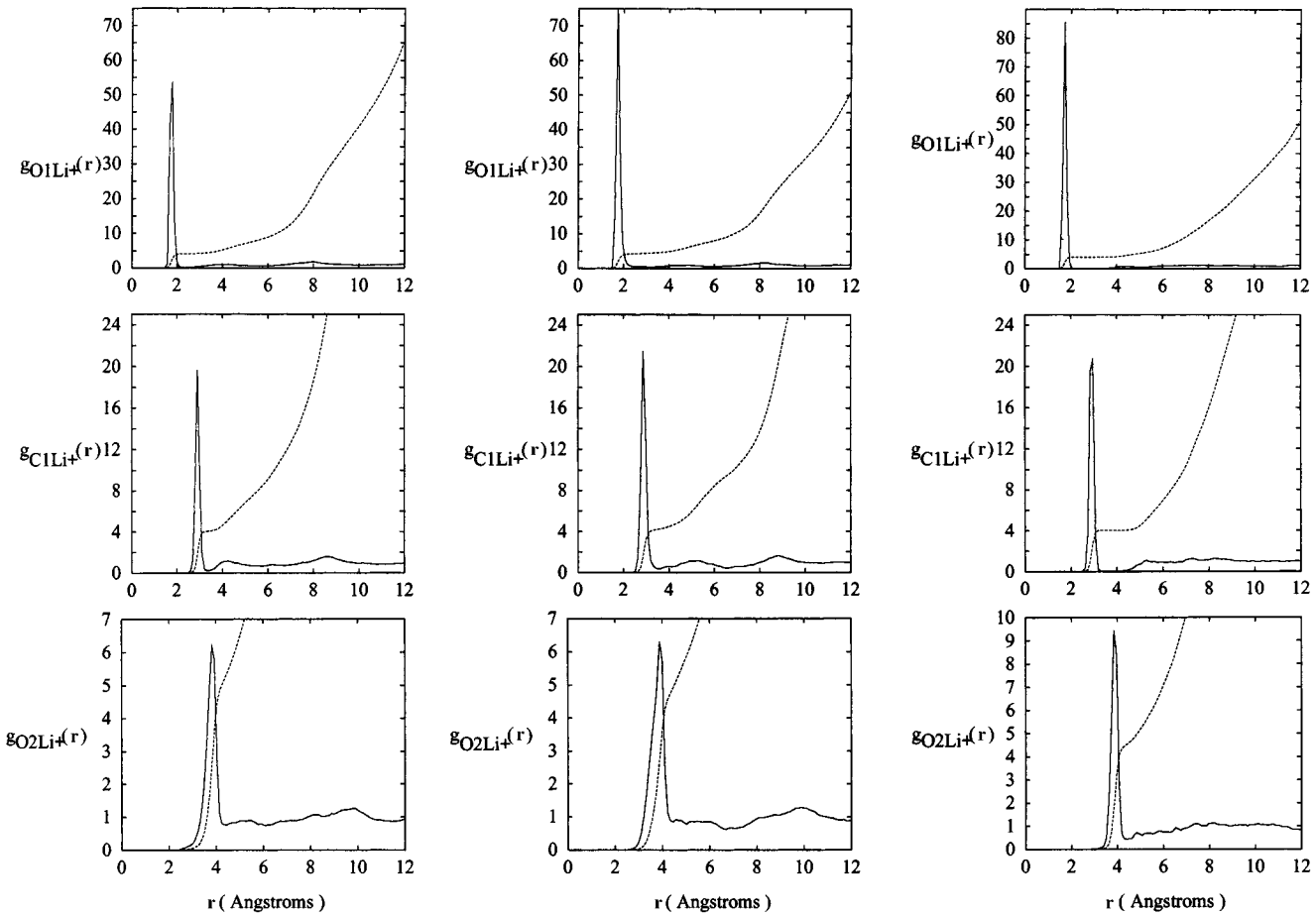

Figure 2. Some carbonate atom−Li^+ ion radial distribution functions (solid line) and running coordination numbers (dashed line). Left column: EC atom−Li^+ (323 K). Middle column: PC atom−Li^+ (323 K). Right column: DMC atom−Li^+ (298 K).

with B−F and F−F distances equal to 1.39 and 2.27 Å, respectively.

NEV molecular dynamics simulations were performed for one Li^+ and one BF_4^- ion in a cubic box containing 214 solvent (EC, PC, or DMC) molecules using periodic boundary conditions. The box sizes are given in Table 2. For three of the simulations (at the lowest temperatures for EC and PC solutions), the initial configuration was prepared from a thermalized configuration of the neat solvent at the experimental density (216 molecules) by replacing two molecules by Li^+ and BF_4^- ions. The molarity of each solution lies in fact in the range 0.05−0.07 M. For the simulations at 348 K with EC and 323 K with PC, the starting configuration of the thermalization process was the final one of the simulation of the same solution at the lowest temperature modified by a volume scaling in order to recover the density of the neat liquid. Rethermalization was then carried out afterward for a variable duration with a time step of 1 fs (see Table 2).

Production simulations were performed at 323 and 348 K for $LiBF_4$/EC and at 298 and 323 K for $LiBF_4$/PC to examine the temperature dependence of the ionic diffusion coefficients. The simulation at 298 K in DMC is only 70 ps long. The equations of motions were integrated with the velocity Verlet algorithm,[21] and the bond lengths were kept rigid by employing the algorithm Rattle.[22] The long-range electrostatic interactions were taken into account by the lattice summation of Ladd[23−25] supplemented by the reaction field of a conductor ($\epsilon_{RF} = \infty$). The Ladd expansion is truncated after the term proportional to $1/a^{11}$, where a is the box edge. The LJ interactions are truncated beyond a molecular cutoff distance equal to $a/2$.

The simulations were done with the MDpol package[26] on an IBM SP2 parallel machine (processor 390). One time step in sequential treatment requires 18.2, 30.3, and 25.9 s of CPU time for EC, PC, and DMC solution, respectively. Test calculations with the coarse-grained parallel version of our program have shown that the acceleration factor remains close to the optimum value up to four processors. To optimize our CPU time allocation, all the simulations were done using four processors for which a speedup of 3.8 was obtained.

III. Results and Discussion

A. Structure and Thermodynamics. The simulation results are given in Table 2. The total potential energy is given as well as the interaction energy of each ion with the solvent. For each solution, the ion−solvent energy is mainly electrostatic (about 95%) and close to −1000 kJ/mol in each solvent for Li^+ and −450 kJ/mol for BF_4^-.

Some radial distribution functions (RDFs) $g_{\alpha\beta}(r)$ for Li^+−solvent atom and BF_4^-−solvent atom are shown in Figures 2 and 3. The cumulative coordination number $n_{\alpha\beta}(R)$ of one atom α is obtained from the relation

$$n_{\alpha\beta}(R) = 4\pi\rho_\beta \int_0^R g_{\alpha\beta}(r)\, r^2\, dr \qquad (1)$$

From some appropriate atom−atom RDFs, eq 1 reveals that there are four solvent molecules in the first solvation shell of the lithium ion and 19 or 20 molecules in the case of BF_4^- for the systems studied. This observation is in agreement with the experimental study by Hyodo and Okabayashi[27] of the local

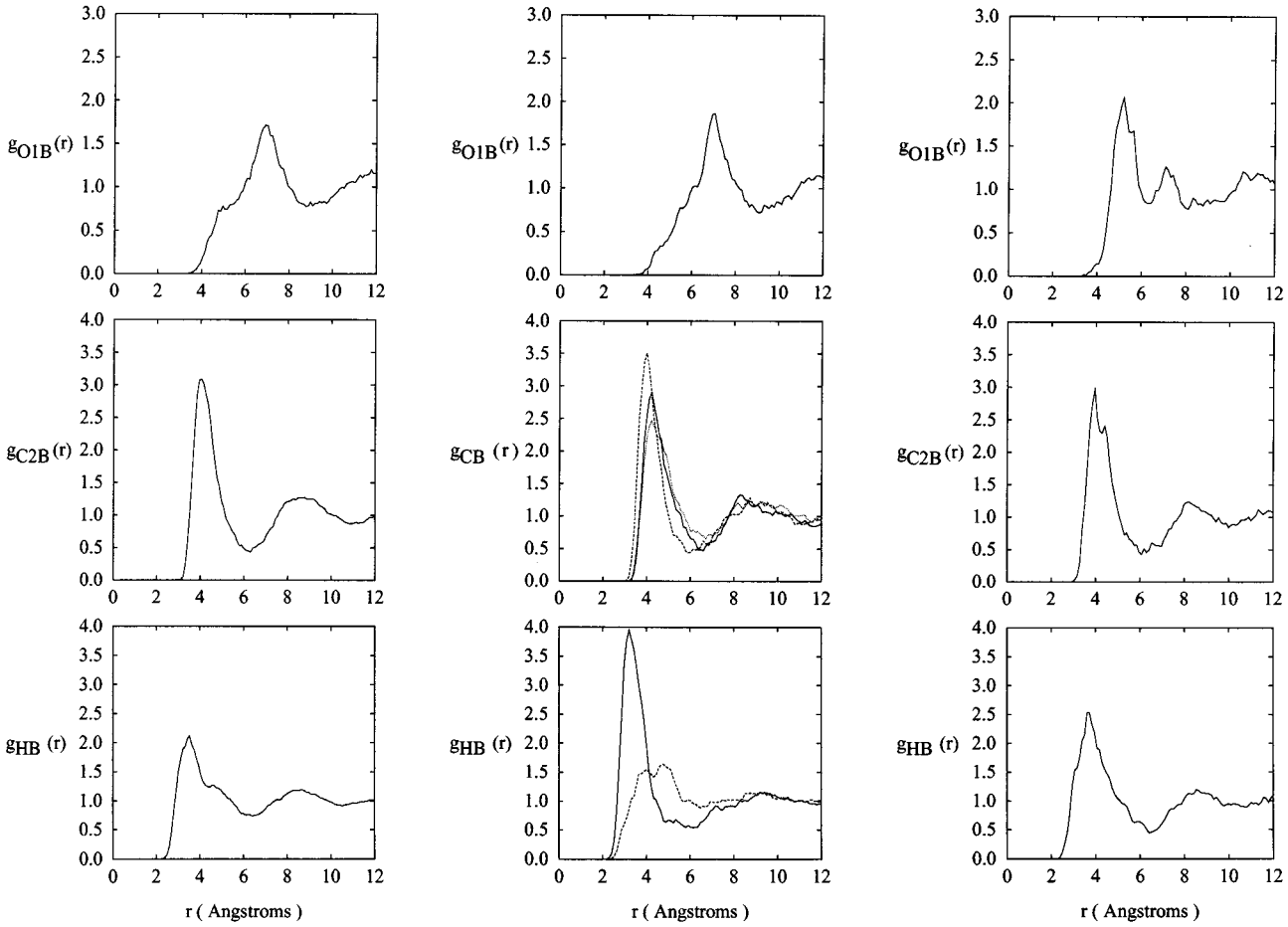

Figure 3. Some carbomate atom−B atom radial distribution functions. Left column: EC atom−B (323 K). Middle column: PC atom−B (323 K). Three curves are given for $g_{CB}(r)$ corresponding to $g_{C4B}(r)$ (solid line), $g_{C10B}(r)$ (dashed line), and $g_{C6B}(r)$ (dotted line). Two curves are given for $g_{HB}(r)$ corresponding to $g_{H10B}(r)$ (solid line) and $g_{HmethylB}(r)$ (dashed line). Right column: DMC atom−B (298 K).

structure of $LiClO_4$ in EC by Raman spectroscopy. These authors have found a coordination number of 4 at 313 K independent of the concentration in the range 0.1−1.0 M. For the system $LiBF_4$/EC, the first peak in g_{O1-Li^+} appears at 1.78 Å with an intensity equal to 55. For the $LiBF_4$/PC and $LiBF_4$/DMC systems, this peak appears at a slightly shorter distance than in EC solvent, and the intensity increases to 75 and 85, respectively. The g_{C1-Li^+} RDF shows that differences occur between the systems for the second solvation shell. For $LiBF_4$/EC, a peak appears at 4.1 Å, whereas for $LiBF_4$/PC it appears at 5.0 Å. For $LiBF_4$/DMC, there is no structure after 5 Å for this RDF. Figure 4 presents typical configurations of the first solvation shell around the Li^+ ion in EC and DMC; for Li^+/PC the picture is very similar to the case Li^+/EC. The distribution function of the angle Li^+−O═C between the line joining the lithium ion and the carbonyl oxygen and the O═C carbonyl bond of the four EC molecules of the first solvation shell of the ion is shown in Figure 5 for the simulation at 323 K; the most probable value is 160°, and similar results are found at 348 K and in $LiBF_4$/PC solution. The flexibility of the DMC molecule exhibits some interesting features. This molecule has two stable conformers, trans−trans (C_{2v}) (shown in Figure 1) and trans−cis (C_s), 13.2 and 13.9 kJ/mol less stable than the trans−trans one from ab initio MP2/6-31G**//HF/6-31G** calculations and from the CFF91 force field, respectively. The C_s conformer (not shown in Figure 1) is obtained by rotating one CH_3 group 180° around the C_1-O_2 (or C_1-O_3) bond. The barrier between both rotamers is equal to 43.2 kJ/mol (MP2/6-31G**//HF/6-31G**) or 36.2 kJ/mol (CFF91). In the liquid phase, nearly all the molecules have the trans−trans geometry. In the first solvation shell of the lithium ion, it is found that roughly two molecules have on average the trans−trans conformation and the two others adopt the trans−cis one. In Figure 6, the fraction of trans−cis DMC molecules as a function of the distance d between the lithium ion and the DMC molecule center of mass is shown. In the first solvation shell ($d \approx 4$ Å), 42% of the molecules are in the C_s conformation on average; as the lithium ion/DMC center-of-mass distance increases, this percentage rapidly falls to approach the bulk value (≈5%) in the second shell ($d \approx 8$ Å). This observation can be understood by noticing that the C_s conformer has a larger dipole than the C_{2v} one (4.11 vs 0.28 D using the partial charge of Table 1), and the strong electrostatic interactions with the lithium charge favor the more polar conformer in the first solvation shell of the lithium ion. In Figure 6, the average fraction of C_s conformer around the BF_4^- ion is also presented, the charge of the ion being spread over a much larger volume; the stabilization of the C_s conformer is much smaller, and only ≈10% of the DMC molecules adopt the C_s geometry in the first solvation shell.

B. Diffusion. The ion diffusion coefficients are computed both from the velocity autocorrelation function (VAC),

$$D^{\mathrm{VAC}} = \frac{1}{3}\int_0^\infty \langle \vec{v}(0)\, \vec{v}(t)\rangle \, \mathrm{d}t \qquad (2)$$

where $\vec{v}(t) = \mathrm{d}\vec{r}(t)/\mathrm{d}t$ is the ion velocity at time t, and from the

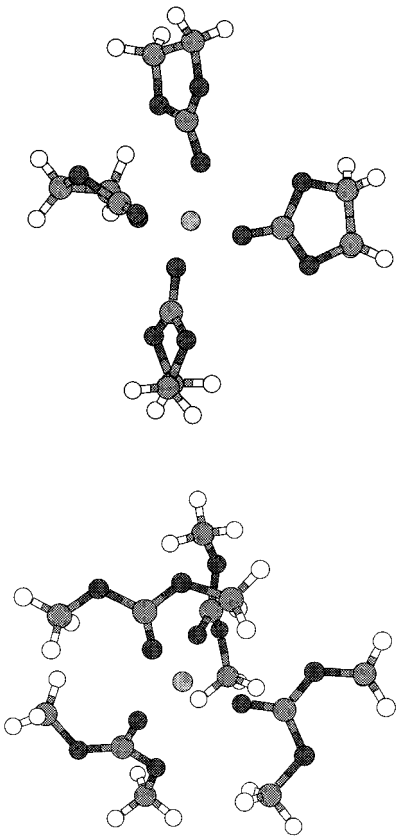

Figure 4. Example of structure of the first solvation shell of EC molecules (top) and DMC molecules (bottom) around the Li^+ ion extracted from molecular dynamics trajectories.

mean square displacement (MSD),

$$D^{\mathrm{MSD}} = \lim_{t\to\infty} \frac{\langle|\vec{r}(t) - \vec{r}(0)|^2\rangle}{6t} \qquad (3)$$

Although both equations are in principle equivalent, insufficient statistical averaging leads to different numerical values in general, the comparison of both determinations being a useful test of convergence of the results. The diffusion coefficients of Li^+ and BF_4^- ions in EC, PC, and DMC are presented in Table 2. The more striking result is that the lithium ion diffuses in a very similar manner in all three solvents; this is linked to the small size of this ion, strongly bound and diffusing with its first solvation shell. Although the simulation times are a bit short to obtain very accurate diffusion coefficient of one ion, we have observed that both VAC and MSD plots (obtained over a 2.5-ps time range) were reasonably well converged. The largest deviation between our VAC and MSD estimates of the ion diffusion coefficient (≈40%) gives a rough estimate of the error bar.

The diffusion coefficient of the lithium ion has been determined experimentally in 0.4 M $LiAsF_6$/PC and 0.6 M $LiAsF_6$/DMC solutions[28] between 298 and 328 K. At 298 K, the experimental value in PC is 0.4×10^{-9} m^2 s^{-1}, very close to our result in dilute solution. At the same temperature, the experimental value in DMC is 0.2×10^{-9} m^2 s^{-1}, a smaller value in DMC than in PC being interpreted by the authors by the presence of contact ion pairs $Li^+-AsF_6^-$ and solvent-separated ion pairs $Li^+(DMC)_4- AsF_6^-$, which do not occur in PC, a much more dissociating solvent (the dielectric constant being equal to 64.9 for PC[29] and 3.1 for DMC[30] at 298 K).

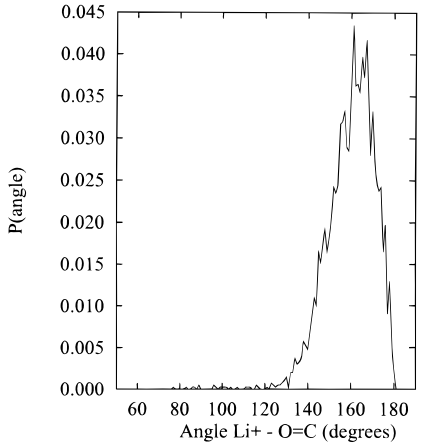

Figure 5. Probability distribution of the angle $Li^+-O{=}C$ for the four EC solvent molecules of the first solvation shell from the molecular dynamics simulation at 323 K.

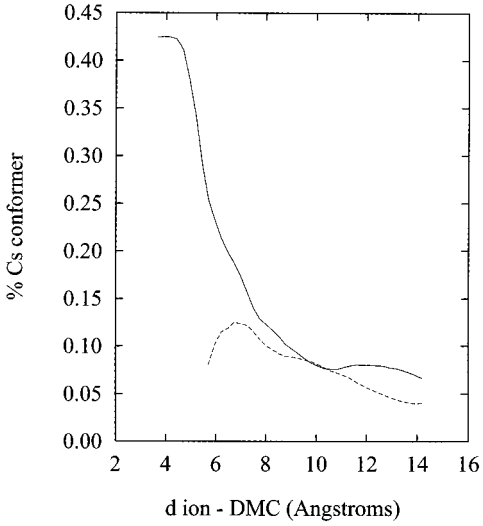

Figure 6. Percentage of DMC molecules in the C_s conformer as a function of the distance between the Li^+ ion (solid line) or the BF_4^- ion (dashed line) and the center of mass of the molecules at 298 K.

For BF_4^-, much less well bound to the solvent molecules of the first solvation shell than Li^+, the diffusion coefficient varies significantly with the solvent, increasing by a factor of ≈5 at 298 K between PC and DMC. In Figure 7, the time evolution of the distance between the lithium ion and the center of mass of the closest eight EC molecules is reported along the 100-ps simulation at 323 K. In these pictures, the fluctuations of the distances d for the four closest molecules are very small, and no exchange of solvent molecules between the first solvation shell and more distant molecules is observed during the whole simulation. These four closest molecules have a diffusion coefficient equal to 0.43×10^{-9} m^2 s^{-1}, which is very close to that of the lithium ion (0.37) and significantly lower than that of the bulk solvent molecules (0.80). All this information confirms the picture of a $Li^+(EC)_4$ complex moving through the solution. Figure 7 presents also similar plots for the eight solvent molecules closest to the BF_4^- ion; in that case the first solvation shell is much less well defined and exchanges of molecules between the first and second solvation shells are frequent.

IV. Conclusion

Molecular dynamics simulations have been used to characterize the local structure and diffusion of Li^+ and BF_4^- ions in

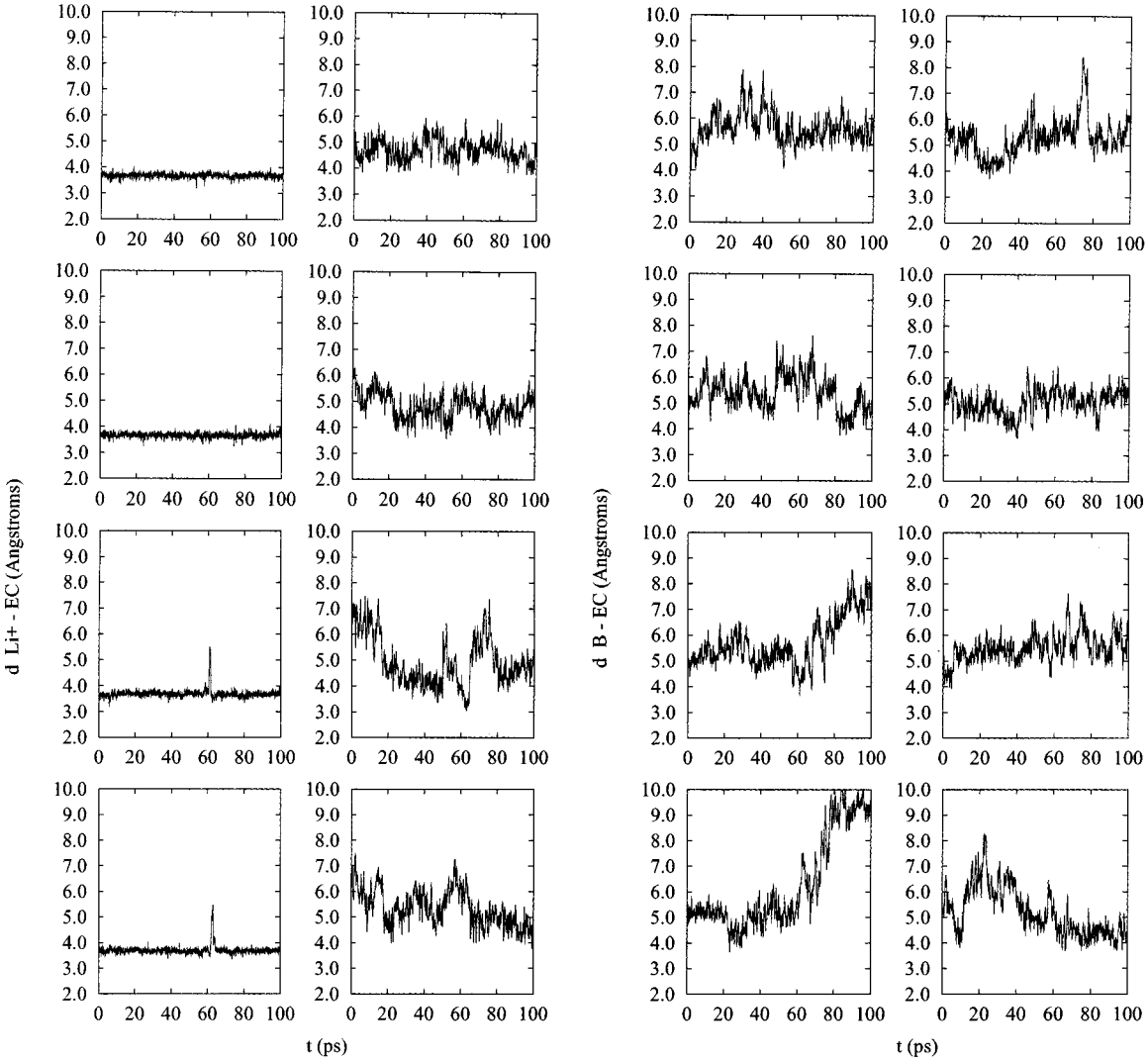

Figure 7. Time evolution of the distance *d* between the Li^+ ion (eight left panels) or the B atom (eight right panels) and the center of mass of the closest height EC molecules at initial time (one graph per molecule) during a 100-ps molecular dynamics simulation at 323 K.

ethylene carbonate (EC), propylene carbonate (PC), and dimethyl carbonate (DMC) at temperatures in the range 298−348 K. In all cases studied, the first solvation shell around the lithium ion is composed of four strongly bound molecules in a tetrahedral arrangement. For dimethyl carbonate solution, it has been found that on average two of the four solvent molecules of the first solvation shell adopt a trans−cis conformation whereas more than 90% have a trans−trans conformation in the bulk. Around the BF_4^- ion, the first solvation shell contains 19 or 20 solvent molecules in all cases. As the average interaction energy of one solvent molecule in the neighborhood of the ion is roughly 10 times larger for Li^+ than for BF_4^-, no exchanges of molecules between the first and the second solvation shell of the lithium ion are observable in 100 ps, whereas many exchanges have been observed in the vicinity of the fluoroborate ion.

The diffusion coefficient of the lithium cation is found to be similar in the three solvents ($(0.3-0.6) \times 10^{-9}$ m^2 s^{-1} in this temperature range), differing by at most a factor of 2 between EC and DMC, with a moderate temperature dependence, and increasing in the order EC < PC < DMC. For BF_4^-, the temperature dependence is more important, and the diffusion of this ion in DMC is much faster than in EC and PC. At 298 K, BF_4^- is found to diffuse faster in PC than in EC.

Acknowledgment. The financial support of the DRET (Paris) (Contract No. 93-2565A) is greatly acknowledged. We thank Sylvie Neyertz and David Brown for useful suggestions. We thank the IDRIS (Paris) and the CNUSC (Montpellier) for the allocation of computer time on an IBM SP2 parallel computer.

References and Notes

(1) Armand, M. B.; Chabagno, J. M.; Duclot, M. J. In *Fast Ion Transport in Solids*; Vashishta, P., Mundy, J. N., Schenoy, G. K., Eds.; Elsevier North-Holland: Amsterdam, 1979.

(2) Aurbach, D.; Gofer, Y.; Ben-Zion, M.; Aped, C. *J. Electroanal. Chem.*, **1992**, *339*, 451.

(3) Impey, R. W.; Madden, P. A.; McDonald, I. R. *J. Phys. Chem.* **1985**, *87*, 5071.

(4) Wilson, M. A.; Pohorille, A.; Pratt, L. R. *J. Chem. Phys.* **1985**, *83*, 5832.

(5) Berkowitz, M.; Wan, W. *J. Chem. Phys.* **1987**, *86*, 376.

(6) Reddy, M. R.; Berkowitz, M. *J. Chem. Phys.* **1988**, *88*, 7104.

(7) Lee, S. H.; Rasaiah, J. C. *J. Chem. Phys.* **1994**, *101*, 6964.

(8) Rose, D. A.; Benjamin, I. *J. Chem. Phys.* **1993**, *98*, 2283.

(9) Mills, G. E.; Catlow, C. R. A. *J. Chem. Soc., Chem. Commun.* **1994**, *18*, 2037.

(10) Neyertz, S.; Thomas, J. O.; Brown, D. *Comput. Polym. Sci.* **1995**, *5*, 107.

(11) Müller-Plathe, F.; van Gunsteren, W. F. *J. Chem. Phys.* **1995**, *103*, 4745.

(12) Müller-Plathe, F.; Liu, H.; van Gunsteren, W. F. *Comput. Polym. Sci.* **1995**, *5*, 89.

(13) Neyertz, S.; Brown, D. *J. Chem. Phys.* **1996**, *104*, 3797.
(14) Carlson, H. A.; Nguyen, T. B.; Orozco, M.; Jorgensen, W. L. *J. Comput. Chem.* **1993**, *14*, 1240.
(15) Chipot, C.; Ángyán, J. G. *GRID Version 3.0: Point Multipole Derived From Molecular Electrostatic Properties*; **1994**, *QCPE 665*, 1994.
(16) Weiner, S. J.; Kollman, P. A.; Nguyen, D. T.; Case, D. A. *J. Comput. Chem.* **1986**, *7*, 230.
(17) Dauber-Osguthorpe, P.; Roberts, V. A.; Wolff, J.; Genest, M.; Hagler, A. T. *Proteins: Struct., Funct., Genet.* **1988**, *4*, 31.
(18) Maple, J. R.; Thatcher, T. S.; Diner, U.; Hagler, A. T. *Chem. Des. Autom. News 5* **1990**, *9*, 10.
(19) Sun, H.; Mumby, S. J.; Maple, J. R.; Hagler, A. T. *J. Am. Chem. Soc.* **1994**, *116*, 2978.
(20) Soetens, J. C.; Millot, C.; Maigret, B. Unpublished work.
(21) Swope, W. C.; Andersen, H. C.; Berens, P. H.; Wilson, K. R. *J. Chem. Phys.* **1982**, *76*, 637.
(22) Andersen, H. C. *J. Comput. Phys.* **1983**, *52*, 24.
(23) Ladd, A. J. C. *Mol. Phys.* **1977**, *33*, 1039.
(24) Ladd, A. J. C. *Mol. Phys.* **1978**, *36*, 463.
(25) Neumann, M. *Mol. Phys.* **1987**, *60*, 225.
(26) Soetens, J. C. Ph.D. Thesis, Université Henri Poincaré−Nancy I, 1996.
(27) Hyodo, S. A.; Okabayashi, K. *Electrochim. Acta* **1989**, *34*, 1551.
(28) Berhil, M.; Chaussé-Tranchant, A.; Messina, R. Submitted to *Electrochim. Acta*.
(29) Payne, R.; Theodorou, I. E. *J. Phys. Chem.* **1972**, *76*, 2892.
(30) *Handbook of Chemistry and Physics, 77*th ed., CRC Press: Boca Raton, FL, 1996.